UNSTEADY VOID MEASUREMENTS WITHIN DEBRIS BEDS USING HIGH SPEED X-RAY TOMOGRAPHY

E. Laurien, T. Stürzel, and M. Zhou

Institute for Nuclear Technology and Energy Systems (IKE),
University of Stuttgart, Germany
Corresponding author: Laurien@ike.uni-stuttgart.de

Abstract

Two-phase flow and boiling within debris beds representing a destroyed reactor core after a severe accident with core fragmentation can be simulated by using the porous media approach. In this approach, a local pressure drop and the heat transfer between the solid debris particles and the two-phase flow is modelled with the help flow-pattern maps, in which the boundaries between bubbly, slug, and annular flow are assumed. In order to support further understanding of these flows we have developed a very fast X-ray measurement device to visualize the 3D-void distribution within particle beds or porous media, which are otherwise un-accessible internally. The experimental setup uses a scanned electron beam directed in circles on a tungsten target to generate the X-rays. The particle bed, which has a diameter of 70 mm, is located between this target and a field of 256 X-ray detectors, which are arranged on a circle concentric to the target. The void distribution is reconstructed numerically from the attenuation of signals, which penetrates the particle bed and the two-phase flow inside. A 3D frame rate of up to 1000 Hz can be reached. The spatial resolution is such that bubbles with a diameter > 1.7 mm can be detected. We have investigated two-phase flows air/water through beds of packed plastic spheres (diameter between 3 and 15 mm) as well as through plastic beds, which were manufactured using a '3D-plotter'. Flow patterns can be individually determined on the basis of empirical criteria. It is confirmed, that the transition between slug and annular flow depends on the air mass flux, but the particle diameter must be considered as an additional parameter.

Keywords: *Two-phase flow, debris bed, porous media, void measurement, x-ray tomography*

1. Introduction

During a severe accident, if the core is not sufficiently cooled due to loss of water, the decay heat of the fission products in the fuel heats up the reactor core. This heat up causes evaporation of cooling water in the core region and decreases the water level in the reactor pressure vessel. The time period of core dryout depends on the accident development and specific reactor design, but the usual time ranges are considered from two to several hours. The decay heat yields a continued heat-

up of the fuel rods and the other core materials. For its modelling flow-pattern maps, pressure drop and heat transfer correlations in porous media are necessary.

In order to analyze the coolability of debris bed, several computational codes have been developed by different institutions e.g. MEWA-code (Buck et al. [1]), ICARE/CATHERE Fichot et al. [2]) and MC-3D (Multi Component-3D, Berthoud [3]) codes developed by IRSN. These codes are still under development to improve the understanding of basic processes related to debris cooling.

For an analysis of long-term coolability i.e. assuming an initially water filled bed heated by decay heat, the modeling of heat transfer between the phases is of minor importance, due to only small deviations from saturation conditions. In this case it is sufficient to assume thermal equilibrium between the phases (solid / liquid). Usually, only small superheats of the particles of few degrees will be required to transfer decay heat to surrounding water. Thus, limitations of cooling do not occur by this process but by limitations of steam removal and especially water access (Bürger and Berthoud [4]). For this condition, the friction forces are decisive for the determination how much water is able enter into the heat-generating bed and how fast the produced steam can be removed.

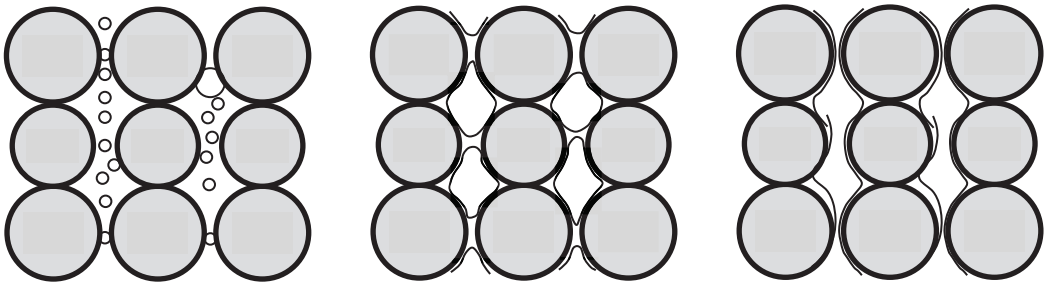

Figure 1. Flow patterns of boiling in a bed of spheres (schematic), representing a nuclear reactor core debris bed

In classical models like the model of Lipinski [5], Reed [6] and Hu & Theofanous [7], interfacial friction is not considered explicitly. In these approaches interfacial friction between steam and water is considered in the relative friction contributions of the phases with the solid, depending on the volume parts. This is not sufficient in general, if interfacial friction between steam and water plays a role. It is not possible to tune the particle fluid drag in the models without interfacial friction to fit the top (counter-current flow) as well as bottom fed (co-current flow) configuration.

An often used approach was proposed by Tung & Dhir [8]. Based on visual observation in air/water experiments, they introduced three different flow regimes, namely bubbly, slug and annular flow regimes. They distinguished the flow regime depending on void fraction as seen in Fig. 1. For each flow regime, individual particle-fluid friction and interfacial friction correlations are derived from geometric considerations.

Tung & Dhir compared their model with the measured pressure gradient and they found a fair agreement with the experiment. But they compared their model with the experiments which are performed with relative large particle diameter. For smaller particle the model results are unsatisfactory (Schmidt [9], Bürger et al. [10]). The range of most interest for reactor applications with respect to severe accidents in LWR lies rather within 1–6 mm diameters. While the values

from the Tung & Dhir model lie significantly below the measured dryout heat flux (DHF) data, especially for sphere diameters smaller than 6 mm.

Some attempts have already been taken by Schmidt [9] to extend the Tung & Dhir model for smaller particles. In his approach, the transition between the flow patterns of bubbly, slug and annular flow have been modified to yield a more rapid transition towards slug and annular flows with smaller particle diameters. Besides the correction of flow patterns the reduction of interfacial friction for the annular flow regime has also been introduced in his approach. But considering these modifications in the Tung & Dhir model, deficit is still detected especially for capturing the DHF results in both top and bottom flooding situations. Thus, the present status of the Tung and Dhir model requires some modifications to extend it for both top and bottom flooding conditions.

In this context the calculations of Rahman [11] demonstrated, that with a modification of the flow-pattern map in the small-particle range yields better results. Of course, this modification is purely empirical and lacks experimental validation.

X-ray computerized tomographic (CT) imaging is a promising approach to investigate industrial, opaque and dynamic processes that can be characterized by density differences. Compared to medical applications, dynamics of the two-phase flow in a debris bed is considerably higher. This makes the achievable frame rate of the CT system an important parameter. Medical electron beam CT (EBCT) e.g. offers frame rates up to 50 frames per second (fps) [12]. Requirements for industrial CT imaging are well above this performance, as frame rates over 1000 fps and a spatial resolution of about 1 mm appear to be inevitable. To date, several scientific workgroups have realized tomographic systems that exceed commercially available performance.

We have set up an experimental facility, which has been designed to perform ultrafast two-dimensional (2D) and three-dimensional (3D) electron beam computed tomography [13,14]. As a novelty, a specially designed transparent target enables tomography with no axial offset for 2D imaging and high axial resolution 3D imaging employing the cone-beam tomography principles. The imaging speed is 10 000 frames per second for planar scanning and more than 1000 frames per second for 3D imaging. The facility serves a broad spectrum of potential applications; primarily, the study of multiphase flows, but also in principle nondestructive testing. In order to demonstrate the aptitude for these applications, static phantom experiments at a frame rate of 2000 frames per second were performed. Resulting spatial resolution was found to be 1.2 mm and better.

The aim of the present paper is to demonstrate a new experimental technique for the investigation of two-phase flows in a debris bed with particles of arbitrary shape. As a first step, spherical particles in a two-phase flow of air and water are used. Unsteady void measurements are performed with high-speed tomographic imaging. The data are used to investigate the role of the particle diameter in the definition of flow pattern-dependent friction and heat transfer coefficients of macroscopic porous-medium models. A new method to manufacture the porous medium, using a 3D plotter, is tested.

2. Description of the Facility

The experimental facility [13,14,15] has been built on the basis of a modified electron-beam welding machine. A picture of the mounted device can be seen in Fig. 2. A sectional view of the measurement setup including beam vessel, target, and annular x-ray detector is shown in Fig. 3. An aluminum vessel is used to enclose the vacuum for the electron beam operation. It contains the target and is mounted below the deflection coils and evacuated by a turbo molecular pump attached to the electron gun. Electrons are accelerated by 150 kV of high voltage, focused on the target and steered along it following a circular paths. To protect the setup from accidental electron

bombardment, several guard plates are used. Thermal resistance is assured by the use of molybdenum sheet. The experiment area in the center is protected by multiple circular plates, whereas vessel and beam monitoring are protected by annular plates installed at half vessel height. The resulting slot restricts the electron beam to deflection angles between 7.0° and 10.2°.

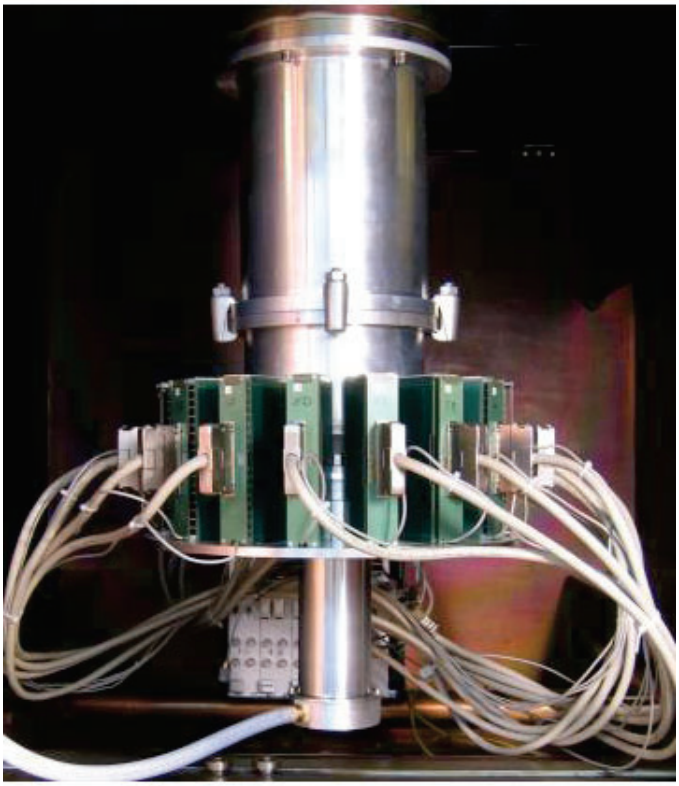

Figure 2: Photograph of the test section with the array of detectors

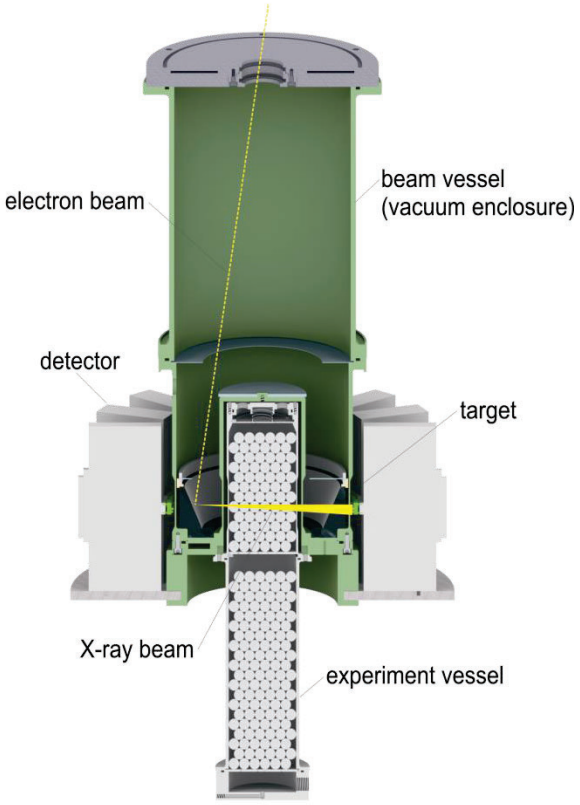

Figure 3: Design modell of the experimental facility with the test section

Due to the specially designed shape of the beam vessel, experiments as well as the fast X-ray detector can be operated under atmospheric conditions. The X-ray detector ring is attached outside of the beam vessel and contains 256 cadmium–zinc–telluride elements.

To perform 2D imaging, the electron beam is deflected in a circular shape. In order to obtain a sufficient quantity of projections per focal spot path, the detector sampling rate has to be a multiple of the deflection frequency. To realize 3D tomography, eight concentric circular xray source paths are generated on the target. The shape of the figure is represented by 4096 discrete points, 512 for each circle. It is produced by a simple QUICKBASIC program and stored in the 32 K EPROM of the deflection generator. Changes in spatial resolution can easily be achieved by programming new beam figures providing a different number of circles. The coated target face is inclined 25° to the beam axis. Since the face does not contain any steps the system is highly flexible concerning adjustment of the main parameters characterizing the spatial and temporal resolutions. For the deflection frequency of 2 kHz, a volume sampling rate of 250 Hz can be obtained.

In order to evaluate the system performance, a number of static and dynamic experiments with a resolution phantom have been conducted. Spatial resolution restricts the temporal resolution and vice versa. The achievable spatial resolution was analyzed by scanning a phantom consisting of

32 different synthetic disks. Each disk contains drillings and grooves of various defined sizes allowing to value spatial resolution. Due to different thicknesses of the slices and an alternately present drilling of diameter 3 mm, axial resolution can be evaluated as well. First pictures are scanned with a deflection frequency of 2000 Hz. The image of a disk containing various drillings and grooves in a range of 1.5–2.2 mm can be seen in Fig. 4.

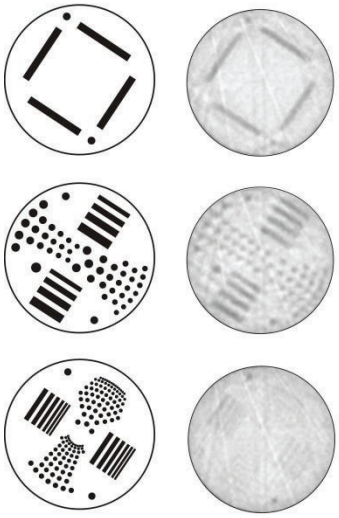

Figure 4: Left: Geometry of various phantoms, right: reconstruction

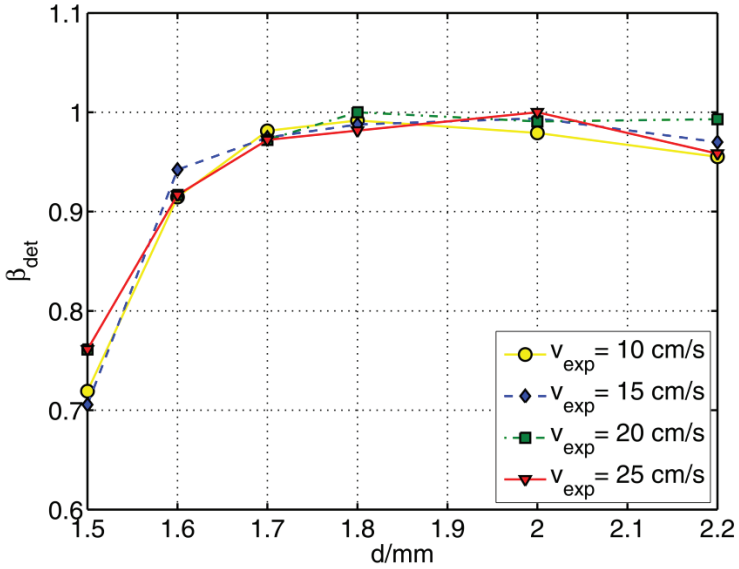

Figure 5: The detection ratio β as a function of the hole diameter for various propagation velocities vexp of the phantoms

The special resolution has been investigated systematically from the data processing algorithm using the reconstruction results of circular drillings after a binarisation based on pixels. A drilling is counted as detected, when it is identified with at least 20% of its area on the phantom. The relative number of detected drillings divided by the number of drillings existing in the phantom is defined as a detection ratio β. It is given in Fig. 5a function of the propagation velocities v_{exp} of the phantoms. It can be seen that the detection ration becomes acceptable (i..e > 0.95 for drillings larger than 1.7 mm).

3. Mesurement Results

3.1 Bed of Spheres

In order to test the capability of this method to recover three-dimensional structures, experiments with a packed bed with polyoxymethylene particles of size 10 mm were performed. The packed bed filled with water was measured, while the dry bed served as a reference. Fig. 6 shows a 3D reconstruction of the resulting water phase between the packed-bed particles. It demonstrates, that a sufficiently large volume can be imaged to capture three dimensional structural changes in the object. The water fraction has been determined to be 0.35, which is quite close to the theoretical value of 0.36. Using a bubble detection algorithm the volume, equivalent diameter and other information can be deduced. Cross sections of arbitrary-arranged spheres of different sizes are shown in Fig. 7.

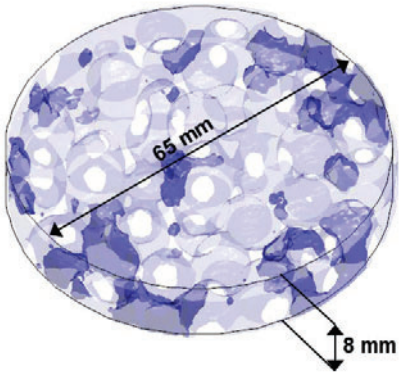

Figure 6: Reconstruction of the void pockets (dark blue) inside a particle bed for d = 10 mm and Jg= 0.1 m/s

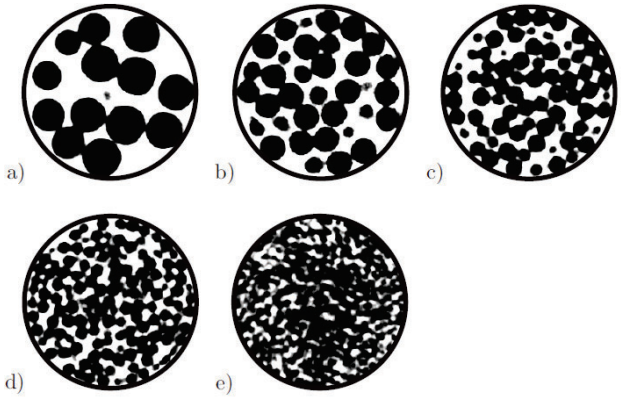

Figure 7: Cross sections of arbitrary packed beds of spheres with various particle sizes, a) 15 mm, b) 10 mm, c) 7 mm, d) 5mm, and e) 3mm

3.2 Empirical Identification of Flow Patterns

From the reconstructed images at various gas superficial velocities and particle sizes, information about the flow patterns can be identified. If the flow pattern is considered to be a bubbly flow, a characteristic bubble size results from the geometrical construction of a bubble, which fits into the gap between perfectly arranged spheres. For 10 mm spheres, this gap is 3.4 mm.

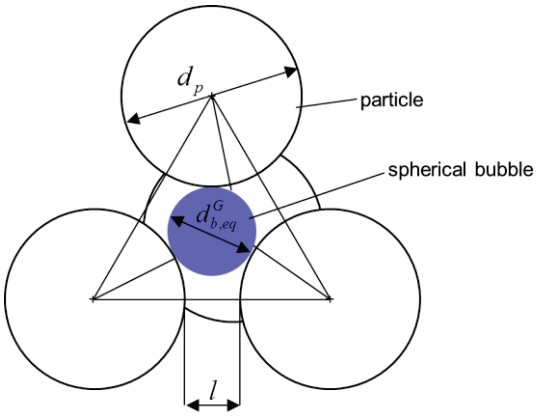

Figure 8: Geometrical consideration for the transition to slug flow by a tetraeder gap

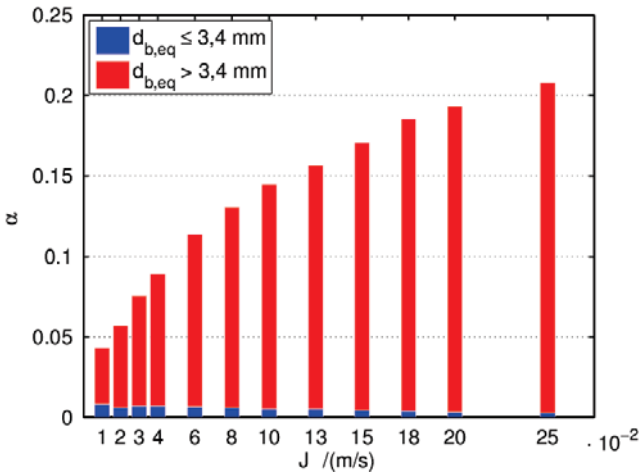

Figure 9: Contribution of small and large bubbles to the void fraction as a function of the gas superficial velocity

After the identification of the bubble size, the tranbsition towards a slug flow, in which bubbles are sonsidered to be larger than the pores, can be investigated. Fig. 9 shows the constribution of bubbles of different sizes on the gas volume flux J. The disctiction between small and large bubbles is based on the characteristic gap size explained above. One can see that

the largest contribution comes from the large bubbles, but there is still a significant contribution from the small bubbles. A clear transition between bubbly flow and slug flow cannot be made on the basis on our criteria, but the potential of our method to support such objective criteria becomes obvious.

Next, the transition from slug flow to annular flow is investigated for various particle sizes. As a basis for an objective criterium, we have defined the contribution of channles in the areea of investigation to the total void fraction. Such channels are denoted as 'stable', when they can be identified throughout the entire measurement time of 3 seconds. In Fig. 11, the increase of the stable part of the void fraction for various particle sizes is shown. Setting an arbitrary threshold, e.g. α_{stable} = 5%, for the transition to annular flow, the average transition void fractions can be extracted. This enables improvement of existing flow regime maps. Generally the novel electron beam device allows for reproducible application of almost arbitrary criteria for the flow characterisation, see Fig. 12.

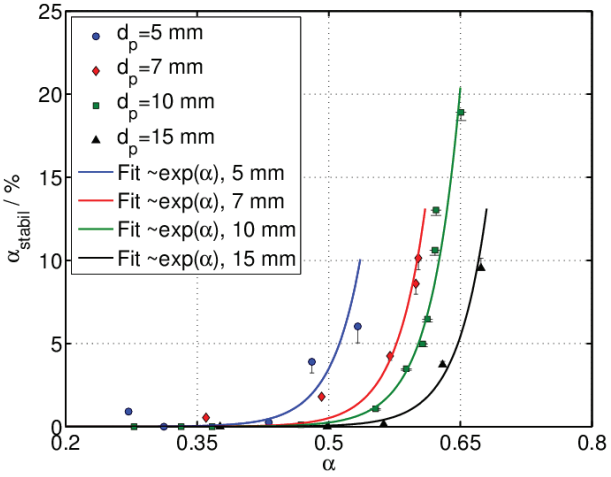

Figure 11: Stable gas fractions for particle diameters d_p = 5,7,10,15 mm at superficial gas velocities of J_g = 0.1 - 0.9 m/s.

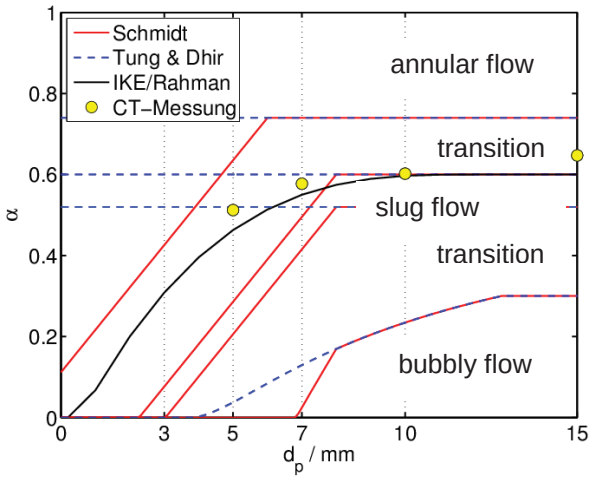

Figure 12: Flow-pattern map of [8] (- - - -), modification of Schmidt [9] (____) and present data (°)

3.3 Bed of Spheres manufactured by 3D-plotter

In order to avoid the boundary influence, a new bed with the closest regular spheres arrangement (Fig. 13 a)) has been manufactured by 3D-plotter. This bed is made of 3 layers of 10 mm spheres. The first and the last layers are identical. There is a sphere in the conter of the layer (Fig. 13 b)). In the conter of the second layer, there is only a free channel because of the arrangement. The bed is 27 mm high. The diameter of the bed is 65 mm. Around the bed, there is a 1 mm shell. After design of the bed by using Autodesk Inventor, the bed has been manufactured through the selective laser sintering method. The material of the bed is PA12 (polyamide).

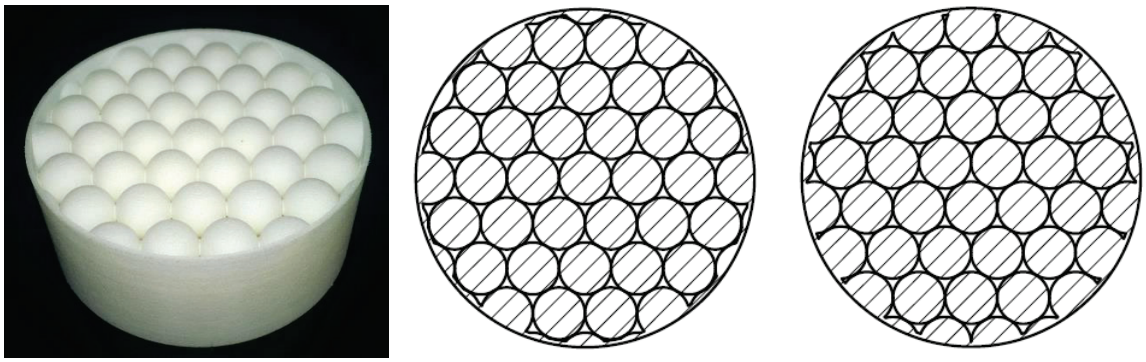

Figure 13: a) Photograph of the manufactured geometry resembling a bed of spheres without boundary influence, b) ,c) two cross section from the design

For identification of the scanning area, a J-needle has been put into the bed from the bottom. According to the image of the J-needle and the arrangement of the spheres, it is possible to know the vertical position of the scanning area (Fig. 14).

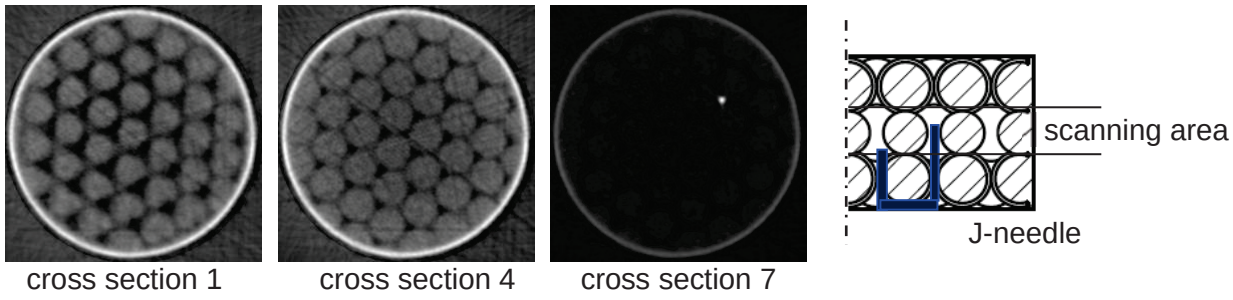

Figure 14: Two-dimensional tomographic of the dry bed with embedded J-needle to identify of the vertical position of the scanning area

Fig. 15 shows the CT images from a measurement of the 2-phase-flow in the 3D bed. The gas flow through the bed is 100 l/min. All the 8 cross sections are showed in Fig. 15. The time step between the first and the forth shooting is 0.45 sec. During the comparison between the two shootings, one can find that most of the channels stay open, but some of them have been closed or reopened by water. That means mostly annular flow and partly slug flow exist in the canning area.

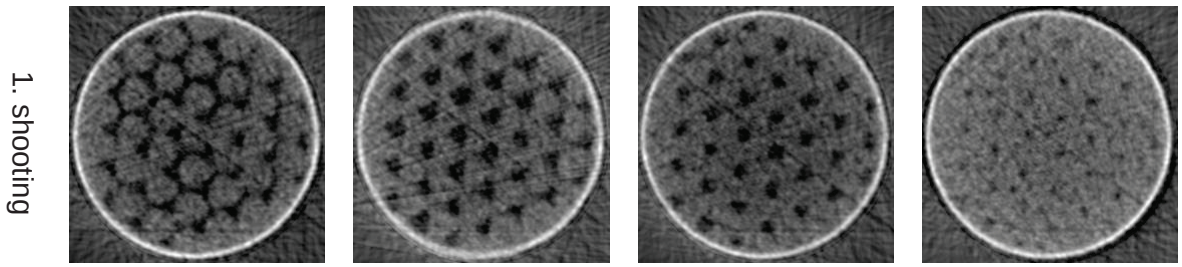

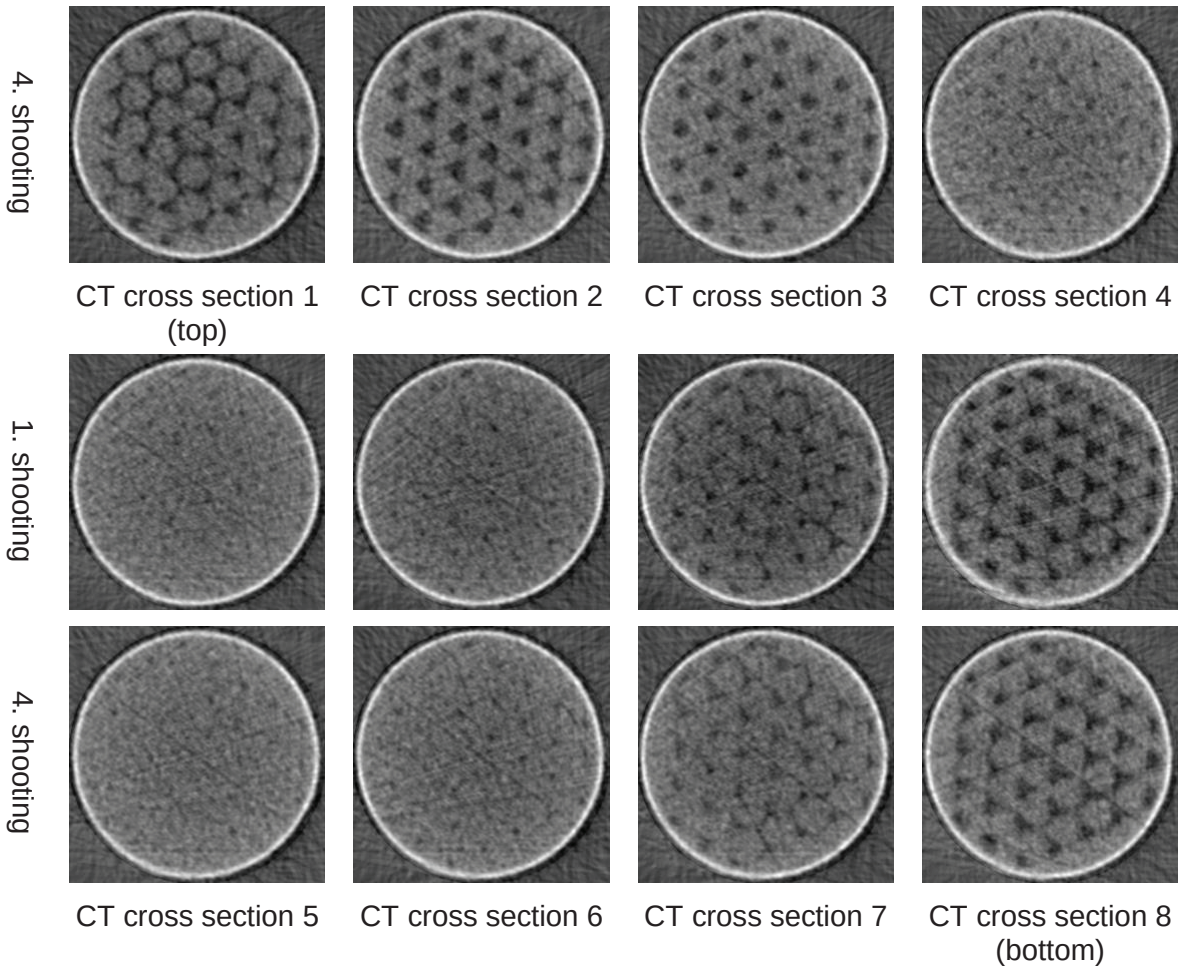

Figure 15: CT images from a measurement with gas flow of 100 l/min

The 3D plotter is useful and valuable. Through the 3D plotter, the geometry, the configuration, the arrangement, the material and the porosity of the scanning object can be easily set up according to the aims of the different works.

4. Summary and Conclusion

High-Speed tomographic imaging and x-Ray tomography is used to identify flow patterns in a bed of spheres. It is confirmed, that the transition between slug and annular flow depends on the air mass flux, but the particle diameter must be considered as an additional parameter. The effects of a finite bed of spheres can be eliminated by manufacturing the porous structures using a 3D-plotter. This technique will enable the investigation of two-phase flows in porous media of almost arbitrary shape.

5. Acknowledgement

This work was supported by the German Science Foundation, LA 553/17-3.

6. References

[1] M. BUCK, M. BÜRGER, S. RAHMAN, G. POHLNER: Validation of the MEWA Model for Quenching of a Severely Damaged Reactor Core, Joint OECD/NEA EC/SARNET2, Workshop on In-Vessel Coolability, Paris, France, October 12 – 14, 2009

[2] F. FICHOT, F. DUVAL, N. TREGOURES, C. BECHAUD, M. QUINTARD: The impact of thermal non-equilibrium and large-scale 2D/3D effects on debris bed reflooding and coolability, Nucl. Eng. Des. 236, 2144-2163 (2006)

[3] G. BERTHOUD: Models and validation of particulate debris coolability with the code MC3D REPO, Nucl. Eng. Des. 236, 2135–2143 (2006)

[4] M. BÜRGER and G. BERTHOUD : Basic laws and coolability of particulate debris: comments on the status and present contributions, Nuclear Engineering and Design, 236: 2049–2059 (2006).

[5] R. J. LIPINSKI: A Model for Boiling and Dryout in Particle Beds. Sandia National Laboratories, SAND 82-9765, NUREG/CR-2646 (1982)

[6] A. W. REED: The effect of channeling on the dryout of heated particulate beds immersed in a liquid pool, PhD Thesis, Massachusetts Institute of Technology, Cambridge, MA (1982)

[7] K. HU, T. G. THEOFANOUS: On the measurement of dryout in volumetrically heated coarse particle beds, Int. J. Multiphase Flow 17, 519–532 (1991)

[8] V. X. TUNG, V. K. DHIR: A hydrodynamic model for two-phase flow through porous media, J. Multiphase Flow14, 47–65 (1988)

[9] SCHMIDT, W., Interfacial drag of two-phase flow in porous media,Int. J. Multiphase Flow, Vol.33, No. 6, pp. 638-657, 2007

[10] M. BÜRGER, M. BUCK, W. SCHMIDT, W. WIDMANN: Validation and application of the WABE Code: Investigations of constitutive laws and 2D effects on debris coolability, Nucl. Eng. Des. 236, 2164-2188 (2006)

[11] S. RAHMAN: Coolability of Corium Debris under Severe Accident Conditions in Light Water Reactors, Dissertation, University of Stuttgart, IKE-2 155 (2013)

[12] D. P. Boyd and M. J. Lipton, "Cardiac computed tomography", Proc. IEEE 71, 298, 1983

[13] F. FISCHER, U. HAMPEL: Ultrafast electron beam X-ray computed tomography for two-phase flow measurement, Nuclear Engineering and Design 240, 2254-2259 (2010)

[14] T. STÜRZEL, M. BIEBERLE, E. LAURIEN, U. HAMPEL, F. BARTHEL, H.-J. MENZ, H.-G. Mayer: Experimental facility for two- and three dimensional ultrafast electron beam x-ray computed tomography, Review of Scientific Instruments 82 (2011)